Journal of
MATERIALS RESEARCH

Preparation of NiFe$_2$O$_4$ powder by spray pyrolysis of nitrate aerosols in NH$_3$

Hsuan-Fu Yu
Chemical Engineering Department, Tamkang University, Taipei Hsien, Taiwan 25137, Republic of China

Ahmed M. Gadalla[a)]
Chemical Engineering Department, Texas A&M University, College Station, Texas 77843

To avoid the formation of hollow spheres during spray pyrolysis, NH$_3$ was employed to change the mechanism of forming NiFe$_2$O$_4$ from aerosols, containing Ni(II) and Fe(III) nitrates in the required stoichiometric ratio. Nearly spherical, solid submicron NiFe$_2$O$_4$ particles with narrow size distribution were produced in one step using a dilute aqueous solution at pyrolysis temperatures as low as 823 K. However, higher pyrolysis temperatures ($\geq$1023 K) reduced the oxides to metallic alloy of Ni and Fe due to dissociation of NH$_3$. The forming steps and possible reaction mechanisms for aerosol droplets involved in the process were discussed.

I. INTRODUCTION

Spray pyrolysis for ceramic powder preparation has attracted the attention of researchers. This technique is also known in the literature[1–5] as the Ruthner process, evaporative decomposition of solution (EDS), and the thermal reaction of atomized solution process (TRAS). Recent studies and development showed that spray pyrolysis can produce fine spherical particles with narrow size distribution, high purity, and high homogeneity. However, the experimental results obtained from our previous studies[6–8] and others[2–5] indicated that in most cases the aerosol-derived particles were hollow spheres as a result of the following steps: (i) evaporation of solvent from the droplets, causing the size reduction and creating a concentration gradient, with the highest solute concentration on the droplet surface; (ii) precipitation of solute on the droplet surface; (iii) formation of solid crust with high porosity; (iv) decomposition of formed solute crust, accompanying the diffusions of gaseous product through the porous crust, and/or sealing of open-connected pores to form impermeable skins; and (v) crystallization and sintering of formed spheres whenever melting points were not reached. Although hollow particles with a thin crust are suitable for production of low density insulating materials or can be used as chemical catalyst supports, they have poor mechanical, electrical, and magnetic properties, and cause a great deal of shrinkage after sintering.

Ingebrethsen *et al.*[9] introduced water vapor into the aerosol process to react with the aerosol droplets of mixed aluminum-titanium alkoxides. The liquid droplets were formed, using the evaporation-condensation method, and hydrated in a heated tube, resulting in the production of noncrystalline, uniform, submicron spheres of mixed aluminum-titanium hydroxides. On the other hand, Clearfield *et al.*[10] atomized the alcoholic solution of mixed Ni(II) and Fe(III) methoxides, hydrated, and then fired in a streamline tubular reactor. Submicron, spherical NiFe$_2$O$_4$ particles were obtained for pyrolysis temperatures up to 843 K. In this study, ammonia (a reacting gas) was introduced into the spray pyrolysis process to react with the generated nitrate aerosol droplets. This reacting gas is expected to change the corresponding reactions and forming mechanism of aerosol-derived particles, resulting in the production of solid particles.

II. EXPERIMENTAL TECHNIQUES

Figure 1 is the spray pyrolysis process used in this study. Nickel nitrate hexahydrate of 99.7% purity and ferric nitrate nonahydrate of 98% purity were dissolved
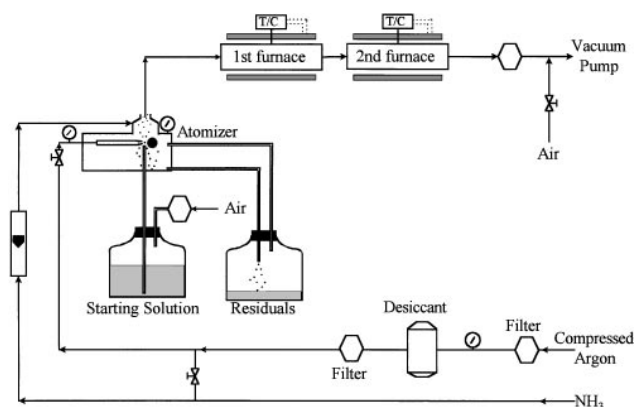

FIG. 1. Schema of the spray pyrolysis process.

in de-ionized water, in the stoichiometric ratio to form NiFe$_2$O$_4$. The solution concentration was determined using the Automatic K-F Titrimeter System (Fisher Scientific Pittsburgh, PA). The six-jet atomizer (Model 9306, Thermal System, St. Paul, MN) used to atomize the solution was modified to allow only fresh solution to be fed into the atomizer, ensuring that the concentration of droplets was always maintained at the predetermined value during operation. The solution was atomized using compressed argon. The generated aerosols carried by argon gas were then introduced into the tubular furnaces to react with NH$_3$ gas, which was injected into the system as shown in Fig. 1. To better control the process and to increase the residence time, two tubular furnaces in series were used. The purpose of the first one is mainly to evaporate the solvent while the second one allows for solid-state reactions. Each tubular furnace in the process was a 3 cm diameter Vycor glass tube (91 cm in length) encased by two semicircular electric heating units (61 cm in length), operable up to 1500 K. The temperature of each furnace was controlled using an Omega, Model 4001–KC, temperature controller in conjunction with a K-type thermocouple placed at the midlength of the glass tube on the exterior wall surface. The resultant particles were then collected on a Nucleopore membrane with 0.2 μm pore size. To account for the increase in pressure created by collecting the particles, the system pressure was controlled and adjusted using a vacuum pump and an air stream with control valve. To study the effects of operating conditions on the quality of derived particles, the collected powder was characterized using thermal analysis (Model STA-409, Netzsch, Ecton, PA), x-ray diffraction (Rigaku Automatic X-ray Diffraction, Stamford, CT), scanning electron microscopy (JEOL JSM-6400), and apparent density measurement (Mercury Poresizer, Model 9300, Micrometrics). The apparent density measurement (operated at about 2000 atm) was used to determine if the particles were hollow or solid.

It is to be noted that anhydrous ammonia gas in the spray pyrolysis process not only was expected to react with the aerosol droplets at the beginning of the process and to alter the forming mechanism of aerosol derived particles, but also was used partly as a carrier gas. Table I summarized the experimental conditions used in this study.

III. RESULTS AND DISCUSSION

The effect of processing temperature was studied by varying the temperature of the second furnace and keeping the first furnace at 373 K. The starting aqueous solution of 20 wt.% (total solutes) was used and the other parameters were kept constant. Figure 2 reveals the morphologies of particles obtained from the ammonia process using three different pyrolysis temperatures (of

TABLE I. Conditions in the spray pyrolysis experiments.

Starting solution	Aqueous solution of mixed Ni(II) and Fe(III) nitrates in the stoichiometric ratio to form NiFe$_2$O$_4$
Temperature of starting solution	298 K
Total solutes in starting solution	20 wt.% and 4 wt.%
Compressed gas (initial flowrate)	Dry Ar (840 mL/min)
Reacting gas (initial flowrate)	NH$_3$ (3140 mL/min)
Temperature of first furnace	373 K
Temperature of second furnace	823, 1023, and 1223 K
System pressure	1 atm (absolute)

the second furnace): 823, 1023, and 1223 K, respectively. It is clear that the resultant particles obtained at different pyrolysis temperatures have different morphologies, and spherical particles were not developed. At 823 K, the large particles with irregular shapes were obtained. The number of these large irregular particles decreased with increasing pyrolysis temperature. To identify the phase present, the specimens were examined by x-ray diffraction, and their XRD patterns are shown in Fig. 3. The pattern obtained at 823 K consisted of crystalline oxide phases. Since the x-ray peaks for NiFe$_2$O$_4$ and Fe$_3$O$_4$ abut or overlap with those for NiO and Fe$_2$O$_3$, the extent of formation of crystalline spinel phases cannot be quantified. However, the existence of crystalline spinel phases was evidenced by some of the particles being attracted to a magnetic field. It is to be noted that a noncrystalline powder was produced at 823 K when argon gas was substituted for NH$_3$. At 1023 K, Fe$_3$NiN was found to be the major constituent with some NiFe$_2$O$_4$, alloy of Ni and Fe, and a trace of Ni$_4$N. At 1223 K, an alloy of Ni and Fe appeared as the major phase while only a small quantity of Fe$_3$NiN was present.

The thermal behavior of these specimens was studied using a simultaneous thermal analyzer (TGA and DTA) in stagnant air (an oxidizing atmosphere) with a heating rate of 5 K/min (Fig. 4). During heating, the specimen obtained at 1223 K increased in weight first and then leveled off to a constant weight above 923 K. This weight gain was accompanied by exothermic effects, indicating that the metallic alloy oxidized and above 923 K a constant weight was obtained, indicating complete oxidation and formation of NiFe$_2$O$_4$ (which was evidenced by x-ray diffraction analysis). A reversible loss in weight was observed at 1673 K, indicating a slight loss of oxygen and formation of nonstoichiometric ferrite phase as reported in the literature.[11] A similar thermal behavior was observed for the powder collected at pyrolysis temperature of 1023 K with a constant weight achieved at a lower temperature. For

664

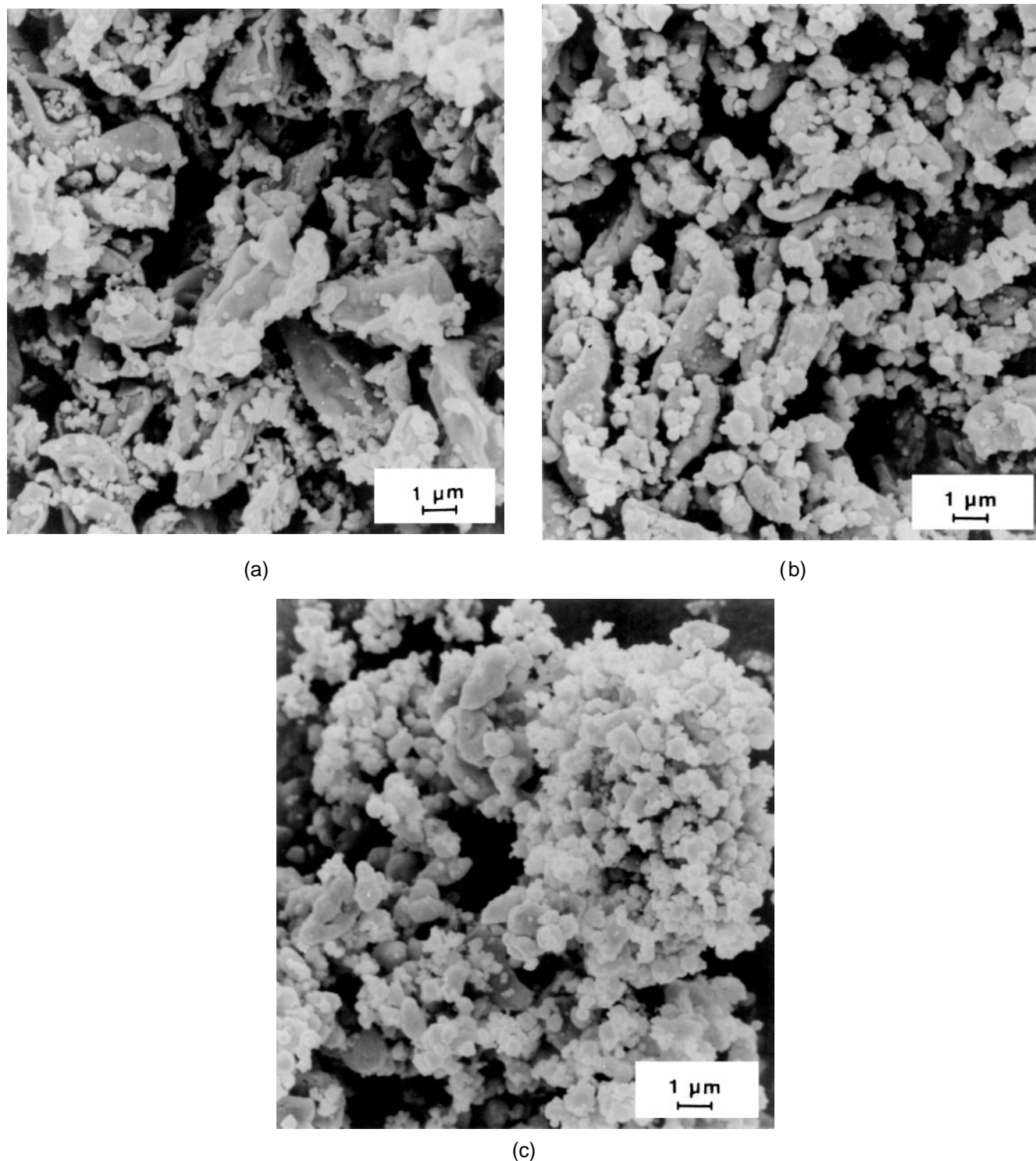J. Mater. Res., Vol. 11, No. 3, Mar 1996

FIG. 2. SEM photomicrographs for particles obtained at pyrolysis temperatures (second furnace) of (a) 823 K, (b) 1023 K, and (c) 1223 K, using 20 wt.% (total solutes) starting solution.

the powder produced at 823 K, an insignificant change in weight was observed.

To investigate the intermediate changes in particle morphologies during thermal treatment, the particles obtained at 823 and 1223 K were heated to 1073 K in stationary air at 5 K/min, followed by cooling to room temperature using the same rate. The fired specimens were then characterized. The results obtained from thermal analysis and x-ray diffraction showed that these fired specimens were all well-crystallized NiFe$_2$O$_4$. The

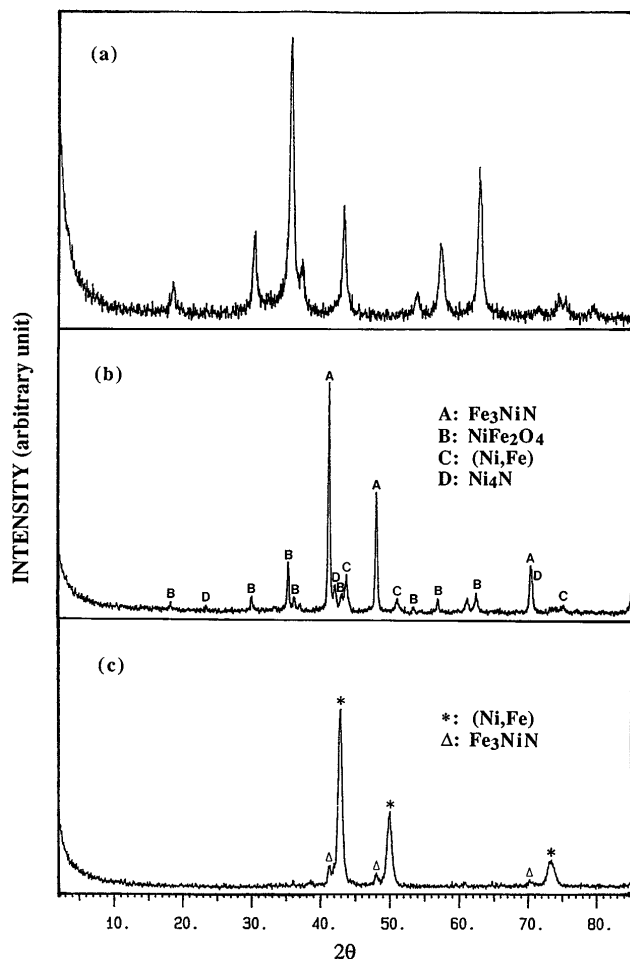J. Mater. Res., Vol. 11, No. 3, Mar 1996

665

FIG. 3. XRD patterns for particles obtained at pyrolysis temperatures (second furnace) of (a) 823 K, (b) 1023 K, and (c) 1223 K, using 20 wt. % (total solutes) starting solution.
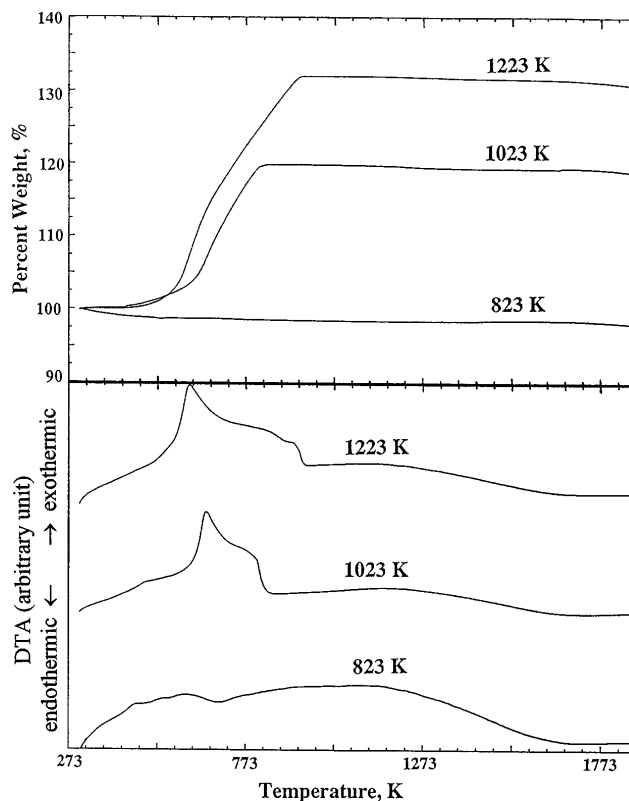

FIG. 4. Thermal curves for particles obtained at pyrolysis temperatures (second furnace) of 823 K, 1023 K, and 1223 K, using 20 wt. % (total solutes) starting solution.

morphology of fired particles obtained at 823 K (metal oxides) showed slight agglomeration and sintering [compare Fig. 5(a) with Fig. 2(a)]. However, this thermal treatment caused the powder obtained at 1223 K (mainly metallic alloy) to produce much smaller particles [compare Fig. 5(b) with Fig. 2(c)]. This size reduction is believed to be due to the nucleation of a new phase and/or the high stresses created by the increase of specific volume, resulting from the oxidation of Fe₃NiN and (Ni, Fe) solid solution to form NiFe₂O₄. By comparing the apparent density, determined by mercury porosimeter (operation pressure at 2000 atm), to that of NiFe₂O₄ (5.4 g/cm³),[12] it was concluded that the fired specimen (heating to 1073 K) consists of solid particles. Although the powder produced at 1223 K followed by heating in air to 1073 K was not spherical, it consisted of pure, well-crystalline, solid NiFe₂O₄ submicron particles with very narrow size distribution [Fig. 5(b)].

To study the effect of solute concentration, a dilute aqueous solution of Ni(II) and Fe(III) nitrates, containing 4 wt. % total solutes, was used as the starting solution, and results were compared with those obtained using a solution having 20 wt. % (total solutes). The morphologies of the products obtained by adjusting the second furnace temperature to 823, 1023, and 1223 K are revealed in Fig. 6. The large irregular particles no longer appeared in these specimens, but tiny spherical particles with dimensions of 1 μm or less were produced. It seems that with a dilute solution, a continuous solid skin failed to form on the droplet surface and discrete islands of solid precipitates were formed. After evaporating the remaining solvent, these precipitated clusters disintegrated into tiny particles. The increase of processing temperature caused the clusters of tiny particles to undergo not only the reduction reaction, but also partial sintering, resulting in an increase of particle size. X-ray diffraction analysis showed that the phases existing in these three specimens were the same as those obtained using 20 wt. % aqueous solution, but much smaller crystals were produced as evidenced from the broader peaks obtained by x-ray diffraction. It is to be noted that all the particles obtained at 823 K, using a dilute starting solution, showed magnetic properties, indicating that the particles at 823 K contained crystalline NiFe₂O₄. The powder produced at a pyrolysis temperature of 1223 K is
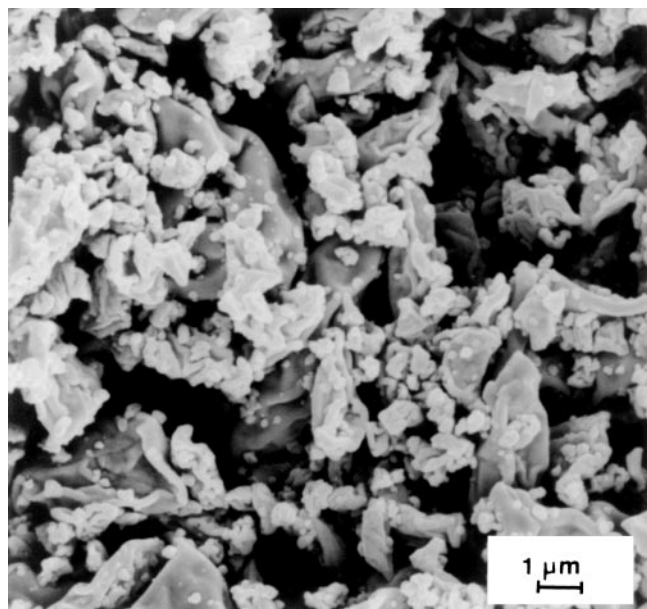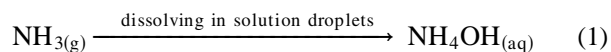
(a)
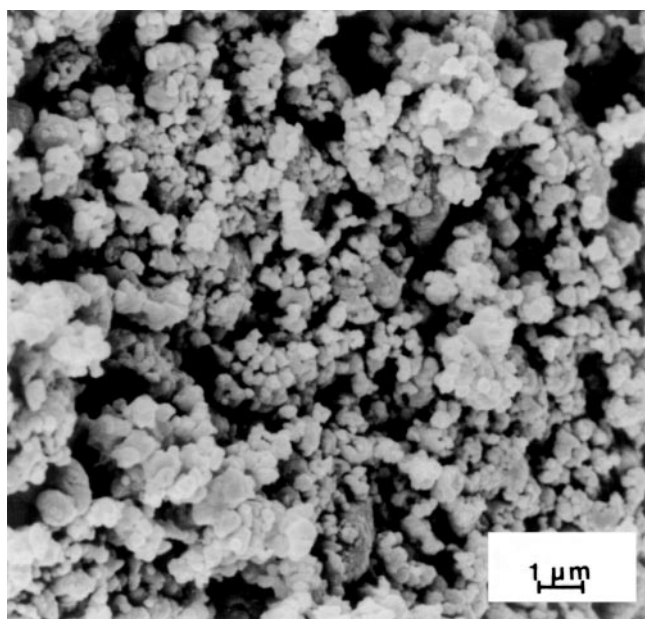
(b)

FIG. 5. SEM photomicrographs for fired specimens (heating up to 1073 K in air) of derived particles obtained at pyrolysis temperatures (second furnace) of (a) 823 K and (b) 1223 K.

expected to be reduced in size after the thermal treatment at 1073 K in air, as shown for the specimens from the higher concentration.
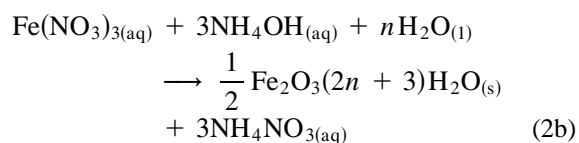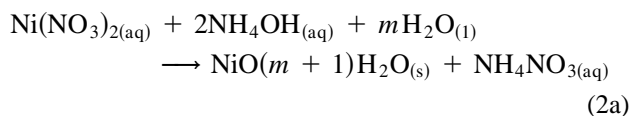
For the sake of comparison, Fig. 7 shows particles obtained from the process mentioned above, under the same operating conditions but using an inert gas of argon, instead of a reacting gas of NH$_3$, at a pyrolysis temperature of 1223 K. The particles in Figs. 7(a) and 7(b) were produced using the starting solutions contain-

ing total solutes of 20 wt. % and 4 wt. %, respectively. While the x-ray diffraction showed that these particles were crystalline NiFe$_2$O$_4$, the measured apparent density (ranging from 3.0 to 4.0 g/cm^3) indicated that hollow spheres were formed. It is clear that the ammonia process produced NiFe$_2$O$_4$ powder having a much higher quality.
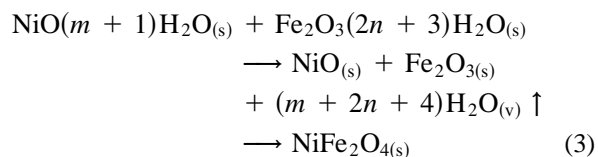
Based on the results mentioned above and the x-ray diffraction pattern for an intermediate product collected from the ammonia process at 373 K (the XRD pattern showed the existence of crystalline NH$_4$NO$_3$), the following chemical reaction mechanism are speculated for the aerosol during spray pyrolysis:
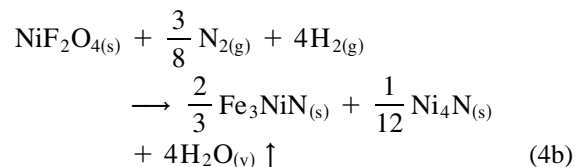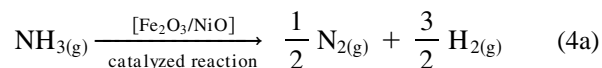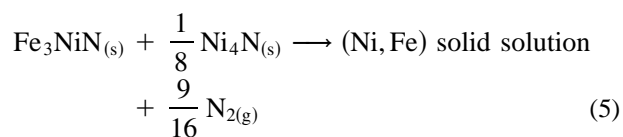Step 1:

$$NH_{3(g)} \xrightarrow{\text{dissolving in solution droplets}} NH_4OH_{(aq)} \quad (1)$$

Step 2:

$$Ni(NO_3)_{2(aq)} + 2NH_4OH_{(aq)} + m H_2O_{(1)}$$
$$\longrightarrow NiO(m + 1)H_2O_{(s)} + NH_4NO_{3(aq)} \quad (2a)$$

$$Fe(NO_3)_{3(aq)} + 3NH_4OH_{(aq)} + n H_2O_{(1)}$$
$$\longrightarrow \frac{1}{2} Fe_2O_3(2n + 3)H_2O_{(s)}$$
$$+ 3NH_4NO_{3(aq)} \quad (2b)$$

Step 3:

$$NiO(m + 1)H_2O_{(s)} + Fe_2O_3(2n + 3)H_2O_{(s)}$$
$$\longrightarrow NiO_{(s)} + Fe_2O_{3(s)}$$
$$+ (m + 2n + 4)H_2O_{(v)} \uparrow$$
$$\longrightarrow NiFe_2O_{4(s)} \quad (3)$$

Step 4 (at high temperature):

$$NH_{3(g)} \xrightarrow[\text{catalyzed reaction}]{\text{[Fe}_2\text{O}_3\text{/NiO]}} \frac{1}{2} N_{2(g)} + \frac{3}{2} H_{2(g)} \quad (4a)$$

$$NiF_2O_{4(s)} + \frac{3}{8} N_{2(g)} + 4H_{2(g)}$$
$$\longrightarrow \frac{2}{3} Fe_3NiN_{(s)} + \frac{1}{12} Ni_4N_{(s)}$$
$$+ 4H_2O_{(v)} \uparrow \quad (4b)$$

Step 5 (at higher temperature and/or longer residence time):

$$Fe_3NiN_{(s)} + \frac{1}{8} Ni_4N_{(s)} \longrightarrow (Ni, Fe) \text{ solid solution}$$
$$+ \frac{9}{16} N_{2(g)} \quad (5)$$
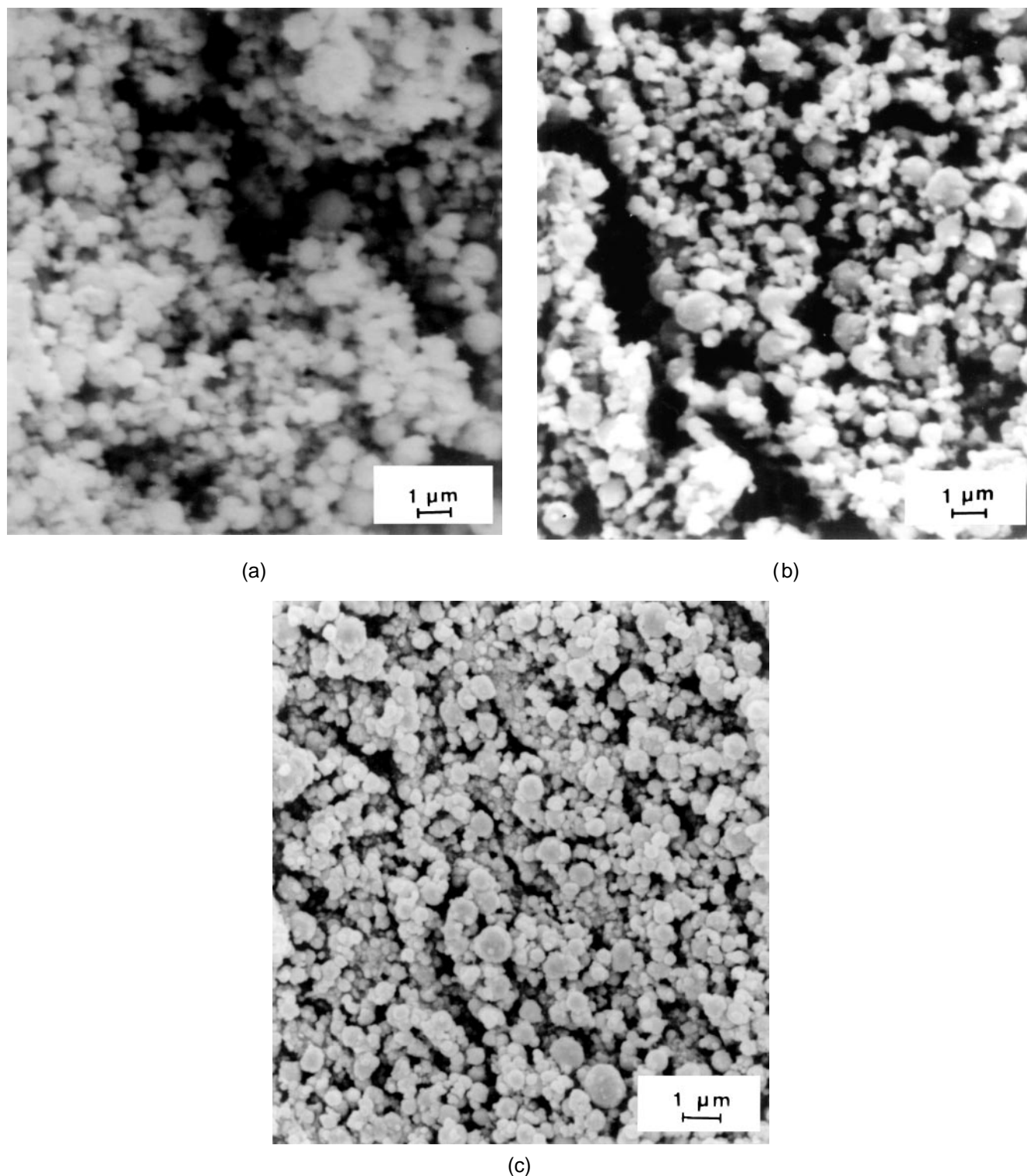
J. Mater. Res., Vol. 11, No. 3, Mar 1996

667

FIG. 6. SEM photomicrographs for particles obtained at pyrolysis temperatures (second furnace) of (a) 823 K, (b) 1023 K, and (c) 1223 K, using 4 wt. % (total solutes) starting solution.

It should be noted that the reactions between the nitrates and NH$_4$OH in the aerosol might not be as simple as those described in step 2. Before forming the corresponding hydrated oxides, some complexes [e.g.,

Ni(NH$_3$)$_x$(NO$_3$)$_2$, with $x = 0-6$] might be present as intermediates, depending on the pH value of the aerosol. However, it would be extremely difficult to predict the local pH conditions in the aerosol since many processes

668

J. Mater. Res., Vol. 11, No. 3, Mar 1996
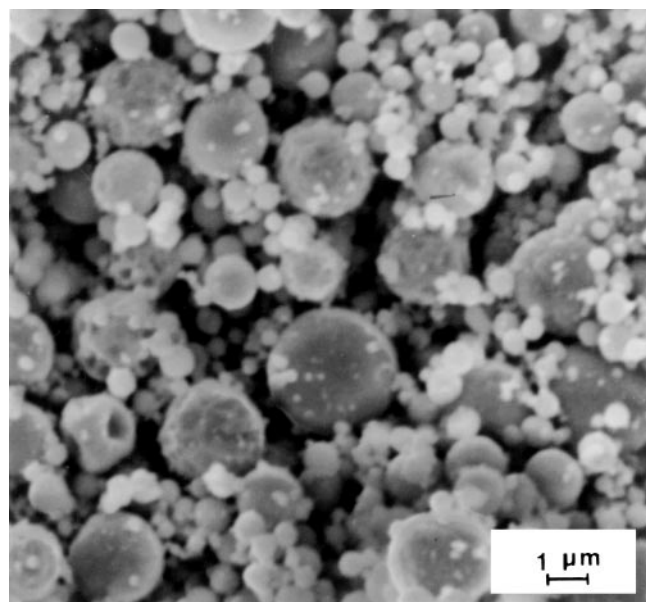
(a)
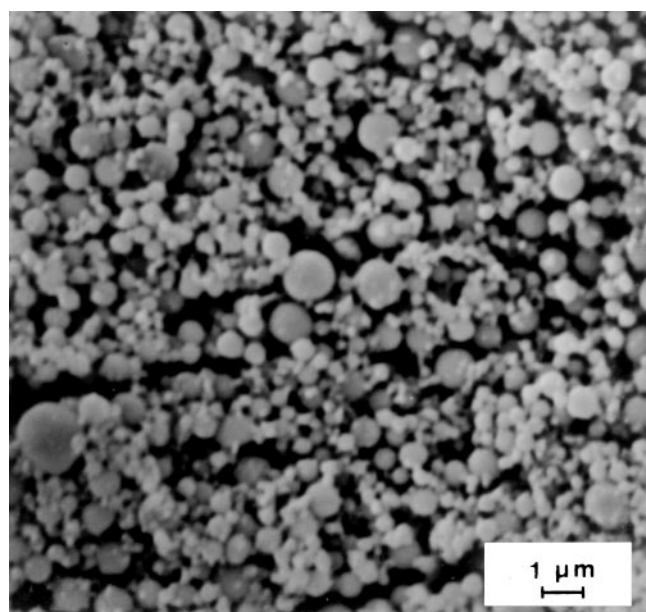
(b)

FIG. 7. NiFe$_2$O$_4$ powder obtained at 1223 K (second furnace) using an inert gas of argon (instead of reacting gas of NH$_3$) with starting solutions of (a) 20 wt.% and (b) 4 wt.% total solutes.

(e.g., NH$_3$ diffusion, solvent evaporation, precipitation, and skin formation) are occurring simultaneously during spray pyrolysis. Here, step 2 is assumed only according to the experimental results obtained in the present work (i.e., the presence of NH$_4$NO$_3$). Clearly, more strictly designed experiments need to be conducted to understand the other possible changes between the nitrate salts and ammonia compound in the process under various operating conditions. On the other hand, the formation of

the nitrides at high pyrolysis temperature (step 4) might result from the direct reaction between NiFe$_2$O$_4$ and NH$_3$, in addition to the reaction described by Eq. (4b). Evolved gas analysis, which was not conducted in the present work, should be able to provide more information about this change.

The changes in morphology are proposed in Fig. 8. The solvent starts to evaporate from the surface of droplet as soon as the aerosol formed. On contact with NH$_3$ gas, NH$_3$ diffuses into the solution droplet and reacts with nitrates. The solute distributed on the surface of droplet will first react with NH$_{3(aq)}$ (or NH$_4$OH) to form the corresponding hydrated oxide and, at the same time, some NH$_{3(aq)}$ will continue to diffuse inward to the center of droplet. It is proposed that at high solute concentration, a continuous pliable solid skin with high porosity forms on the surface of droplet. Because of the interfacial tensions between phases, the surface skin collapses, resulting in a large particle with irregular shape. Since this skin has high porosity, some unreacted nitrate solution will pass through the collapsing skin and react with NH$_{3(aq)}$ to form small solid precipitates
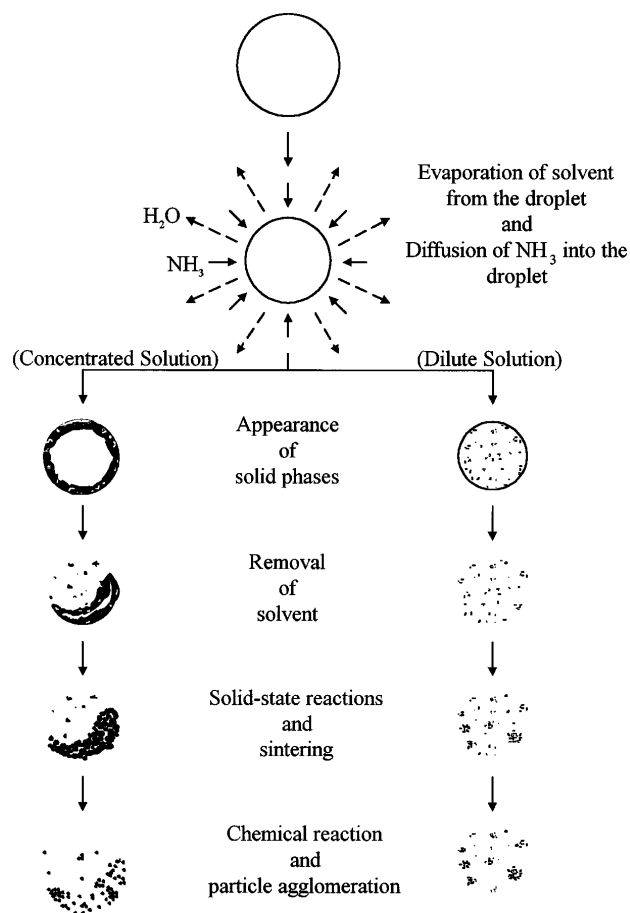

FIG. 8. Forming mechanisms for aerosol-derived particles in the ammonia process.

beyond the collapsed solid skin. Consistent with these steps, a bigger drop of 0.2 cm in diameter was viewed visually and these steps observed. Increasing the pyrolysis temperature enhances the diffusion of ammonia gas into the droplet. Upon further heating, the remaining solvent continues to evaporate and hydrated oxides decompose to the corresponding anhydrous oxides. At high temperature ammonia, presumably catalyzed by existing metal oxides, decomposes to N$_2$ and H$_2$ and provides a reducing atmosphere. The oxides will then form nitrides and reduce to the metallic state, depending on the pyrolysis temperature and the time of contact. These phase changes cause the disintegration of oxide particles to much smaller particles. The shattered nonoxide particles are formed and observed in the particles collected at high pyrolysis temperatures (i.e., using 1023 and 1223 K). These tiny particles are expected to be fairly active. Thermal treatment in air causes the particles to oxidize back to nickel ferrite. Again, because of the nucleation of new phase during oxidation, the particles will be further reduced to form submicron particles.

When a very dilute solution (e.g., 4 wt. % total solutes) is used as starting solution, a continuous solid skin may not be formed on the surface of solution droplet, due to the limited amount of nitrates available on the surface to react with NH$_{3(aq)}$. Small clusters of solid precipitates would then form. During pyrolysis, these small clusters would tend to spheroidize in order to reduce their surface energy. Therefore, spherical submicron particles and agglomerates are produced from this ammonia process when a dilute starting solution is used.

IV. CONCLUSIONS

NH$_3$ altered the forming mechanisms of aerosol derived particles. Solid submicron nickel ferrite particles having a fairly narrow size distribution were produced from the ammonia process at a concentration for the starting aqueous solution as high as 20 wt. % (total solutes). Similar particles are expected to be obtained from this process even at higher initial concentration. The experimental results indicated that the droplets with concentrated solution of nitrates reacted with NH$_{3(aq)}$

(NH$_4$OH). It is suggested that there is the formation of pliable continuous skin on the surface of each droplet. The droplets with these pliable solid skin then collapsed and resulted in larger particles with irregular shapes. At a pyrolysis temperature of 1023 K or above, NH$_3$ furnished a highly reducing atmosphere and the particles shattered, forming crystals of the corresponding nitrides as intermediate phases followed by metallic alloys. Thermal treatment of these mixed phase particles at about 1073 K in air caused the particles to be oxidized, resulting in further disintegration and formation of much smaller particles. Using dilute aqueous solution caused the formation of discrete islands of solid precipitates on the droplet surface. By removing the remaining solvent, submicron spherical solid nickel ferrite powder with narrow size distribution was produced in one step at a pyrolysis temperature as low as 823 K.

REFERENCES

1. M. J. Ruthner, H. G. Richter, and I. L. Steiner, in *Ferrites,* edited by Y. Hoshino, S. Iida, and M. Sugimoto (University of Tokyo Press, Tokyo, Japan, 1971), pp. 75–78.
2. G. L. Messing, T. J. Gardner, and R. R. Ciminelli, Sci. Ceram. **12**, 117 (1983).
3. T. J. Gardner and G. L. Messing, Am. Ceram. Soc. Bull. **63**, 1498 (1984).
4. D. W. Sproson, G. L. Messing, and T. J. Gardner, Ceram. Int. **12**, 3 (1986).
5. D. W. Sproson and G. L. Messing, in *Ceramic Powder Science,* edited by G. L. Messing, K. S. Mazdiyasni, J. W. McCauley, and R. A. Haber (The American Ceramic Society, Inc., Westerville, OH, 1987), pp. 99–108.
6. A. M. Gadalla and H. Yu, J. Mater. Res. **5**, 1233 (1990).
7. A. M. Gadalla and H. Yu, J. Mater. Res. **5**, 2923 (1990).
8. A. M. Gadalla and H. Yu, J. Thermal Analysis **37**, 319 (1991).
9. B. J. Igebrethsen, E. Matijević, and R. E. Partch, J. Colloid Interface Sci. **95**, 228 (1983).
10. A. Clearfield, A. M. Gadalla, W. H. Marlow, and T. W. Livingston, J. Am. Ceram. Soc. **72**, 1789 (1989).
11. W. D. Kingery, H. K, Bowen, and D. R. Uhlmann, *Introduction to Ceramics* (John Wiley & Sons, Inc., New York, 1976).
12. National Institute of Standards and Technology, "Nickel Ferrite (Trevorite), NiFe$_2$O$_4$ (Cubic)", N.I.S.T. Circular 539, Microtext Dept., Texas A&M University, College Station, TX (1960), Vol. 10, p. 44.